Cell PRESS
Immunity
Article

The Sorting Receptor Sortilin Exhibits a Dual Function in Exocytic Trafficking of Interferon-γ and Granzyme A in T Cells

Stefanie Herda,[1] Friederike Raczkowski,[4] Hans-Willi Mittrücker,[4] Gerald Willimsky,[5] Kerstin Gerlach,[1] Anja A. Kühl,[6] Tilman Breiderhoff,[2] Thomas E. Willnow,[2] Bernd Dörken,[1,7] Uta E. Höpken,[3] and Armin Rehm[1,7,*]
[1]Department of Hematology, Oncology and Tumorimmunology
[2]Department of Molecular Cardiovascular Research
[3]Department of Tumor and Immunogenetics
Max-Delbrück-Center for Molecular Medicine, 13125 Berlin, Germany
[4]Institute for Immunology, University Medical Center, 20246 Hamburg-Eppendorf, Germany
[5]Institute of Immunology
[6]Department of Pathology/Research Center Immuno Sciences
Charité-Universitätsmedizin Berlin, 12200 Berlin, Germany
[7]Department of Hematology, Oncology and Tumorimmunology, Charité-Universitätsmedizin Berlin, 13353 Berlin, Germany
*Correspondence: arehm@mdc-berlin.de
http://dx.doi.org/10.1016/j.immuni.2012.07.012

SUMMARY

Immunological control of infections or tumors depends on the release of effector cytokines and polarized secretion of cytotoxic granules from T cells and natural killer cells. Here we show that the sorting receptor Sortilin controlled both processes. In murine Sortilin-deficient cytotoxic T lymphocytes, regulated secretion of granzyme A and cytotoxic killing was enhanced and correlated with increased vesicle-associated membrane protein 7 availability. In contrast, loss of Sortilin reduced the release of interferon-γ upon infections and in autoimmune colitis. Exit of interferon-γ from the Golgi apparatus required the presence of Sortilin. Furthermore, we tracked the transport route of interferon-γ beyond this Sortilin-dependent Golgi to early endosome step. In wild-type T cells, trafficking of interferon-γ from the endosomal sorting platform to the plasma membrane proceeded independently of recycling endosomes, and interferon-γ remained excluded from late endosomes. Our results suggest that Sortilin modulates systemic immune responses through exocytic sorting of immunological effector molecules.

INTRODUCTION

Elimination of virus-infected and tumorigenic cells requires proper cytolytic activity by cytotoxic T lymphocytes (CTL), aided by the cytotoxic response of natural killer (NK) cells and the cytokine response of T helper type 1 (Th1) cells (Russell and Ley, 2002). Cytolytic activity of T cells is determined by their avidity for the major histocompatibility complex (MHC)-peptide ligand, synthesis and storage of effector molecules, intracellular vesicle transport, and maturation of cellular organelles. CTL selectivity requires specific recognition of MHC class I-peptide complexes by the T cell receptor (TCR), which allows the precise delivery of the cytolytic agents perforin and granzymes into the immunological synapse (IS) via the regulated secretory pathway (Fooksman et al., 2010). This process involves storage in and release from lytic granules, also referred to as secretory lysosomes (Stinchcombe et al., 2004; Voskoboinik et al., 2006). In contrast, secretion of the effector cytokines interferon-γ (IFN-γ) and tumor necrosis factor-α (TNF-α) is dependent on the constitutive secretory pathway, where newly synthesized proteins pass through the Golgi apparatus and, upon TCR engagement, are released at the plasma membrane in a protracted manner (Catalfamo et al., 2004; Fortier et al., 1989; Huse et al., 2006). Genetically modified mouse strains or T cells derived from patients with hereditary diseases have provided insight into key mechanisms responsible for the transport and release of granzymes from lytic granules (Stinchcombe et al., 2004). However, there are no in vivo models for the molecular dissection of IFN-γ and TNF-α trafficking pathways from CTLs, Th1 cells, and NK cells.

Here, we examined the cellular machinery that facilitates transport of granzymes and IFN-γ from the trans-Golgi network (TGN) toward their endosomal-lysosomal destination. For cathepsins and granzymes, delivery beyond the TGN to lysosomes is thought to depend on association with cation-dependent and -independent mannose-6-phosphate receptors (CD-M6PR and CI-M6PR) (Ghosh et al., 2003). This complex recruits clathrin adaptors, followed by the formation of clathrin-coated vesicles (CCVs) or carriers that transport the hydrolase-M6PR complex to endosomes. The cargo-receptor complex dissociates in endosomes, the receptor recycles to the TGN, and the hydrolase is targeted to secretory lysosomes. Trafficking steps that regulate IFN-γ anterograde transport to post-Golgi compartments remain to be resolved.

The vacuolar protein sorting 10 protein (Vps10p) receptor Sortilin exhibits structural and functional similarity to the CI-M6PR (Willnow et al., 2008). Both are type I transmembrane receptors

with a cysteine-rich region within the luminal domain, which accounts for the binding of cargo proteins. They also have homologous signal sequences in their cytoplasmic domains that interact with adaptor protein complexes and reside in the same CCVs, which are transported from the TGN to endosomes (Canuel et al., 2008; Mari et al., 2008; Robinson and Bonifacino, 2001).

Here, we provide evidence that Sortilin exhibits a dual role in murine CTLs, NK cells, and Th1 cells. Although the regulated release of granzyme A was enhanced as a result of an alteration of the late endosomal trafficking regulator vesicle-associated membrane protein 7 (VAMP7), loss of Sortilin abrogated the constitutive delivery of IFN-γ from the TGN to early endosomes. Systemically, lack of IFN-γ transport resulted in a compromised immune response toward infectious stimuli and a dampened autoimmune response in inflammatory bowel disease.

RESULTS

Sortilin Expression and Localization

To address the subcellular localization of Sortilin in cells of the adaptive immune system, murine $CD8^+$ T cells were transfected with a Sortilin-GFP fusion protein. The major proportion of Sortilin-GFP localized together with the Golgi marker GM130 and the early endosome marker EEA1 (Figures 1A–1C). In contrast, quantification of colocalization of Sortilin-GFP with the plasma membrane marker CD8 or the lysosomal protease cathepsin D showed only marginal overlap.

In wild-type (WT) mice, Sortilin gene expression was observed in naive (day 0) and activated (day 3, 5) CTLs (Figure 1D). Correspondingly, protein expression was detectable in lysates from naive and activated CTLs (Figure 1E). *Sort1*$^{-/-}$ mice exhibited normal peripheral blood cell counts and *Sort1*$^{+/+}$ and *Sort1*$^{-/-}$ mice displayed comparable numbers and frequencies of lymphocyte subsets ($B220^+$, $CD4^+$, $CD8^+$ and $CD4^+CD25^+$ regulatory T cells) (data not shown).

Improved Allogeneic Cytotoxicity in *Sort1*$^{-/-}$ CTLs and NK Cells

To investigate the role of Sortilin in the secretory pathway, we generated CTLs from *Sort1*$^{+/+}$ and *Sort1*$^{-/-}$ splenocytes. The number and activation status ($CD8^+CD25^+$, >95%) of CTLs were comparable between *Sort1*$^{+/+}$ and *Sort1*$^{-/-}$ animals. Applying enzymatic activity assays, we found that induced secretion of the secretory lysosome marker granzyme A from *Sort1*$^{-/-}$ CTLs was considerably increased compared with WT CTLs (Figure 2A, left). Release of the conventional lysosomal enzyme β-hexosaminidase was unaffected (Figure 2A, right).

Detection of granzyme B in CTL supernatants elicited no measurable difference between WT and *Sort1*$^{-/-}$ CTLs (Figure 2B). In immunoblot analysis, granzyme B exhibited indistinguishable quantities, whereas granzyme A was reduced in *Sort1*$^{-/-}$ CTLs compared with WT CTLs (Figure 2C). Rapid loss of granzyme A in *Sort1*$^{-/-}$ CTLs could be reversed through inclusion of brefeldin A (BFA) or in the presence of the lysosomal acidification inhibitor concanamycin A (Figure 2D). Enhanced release of functionally active granzyme A in *Sort1*$^{-/-}$ mice translated into increased allogeneic cytotoxicity in vitro (Figure 2E). The enhanced killing capacity of *Sort1*$^{-/-}$ CTLs depended on the release of granzyme-containing lytic granules, as shown by the fact that WT and *Sort1*$^{-/-}$ CTLs showed comparable strong reductions in target cell lysis in the presence of concanamycin A (Figure S1A available online). In the presence of the selective granzyme A inhibitor FUT-175 (Poe et al., 1991), allogeneic cytotoxicity of *Sort1*$^{-/-}$ CTLs was diminished (Figure S1B). Conversely, the magnitude of this reduction corresponded to the gain of cytolytic capacity in *Sort1*$^{-/-}$ CTLs (Figure 2E).

NK cells use a similar exocytosis apparatus for the regulated release of cytolytic agents (Stinchcombe et al., 2004). *Sort1*$^{-/-}$ NK cells exhibited enhanced release of granzyme A and improved cytotoxic activity against YAC-1 target cells (Figures 2F and 2G). Taken together, Sortilin deletion improves the in vitro cytotoxicity of CTLs and NK cells, as mediated by enhanced granzyme A activity.

Increased VAMP7 Expression in *Sort1*$^{-/-}$ CTLs

We analyzed the polarization of the lytic granule marker cathepsin D and the Golgi marker GM130 to the site of contact between CTLs and CD3 CD28 antibody-coated microbeads (Figure S2A). Upon encountering microbeads, granule reorientation in conjugated T cells occurred. In such cells, polarized cathepsin D surrounded by GM130 staining toward the T cell-bead interface was observed. Similar frequencies of conjugates demonstrated tight polarization of lytic granules toward the IS (Figure S2B). Thus, Sortilin does not affect IS formation.

In immunoblot analysis of *Sort1*$^{+/+}$ and *Sort1*$^{-/-}$ $CD8^+$ total lysates, comparable protein amounts were observed for several soluble-N-ethylmaleimide-sensitive-factor accessory-protein receptors (SNAREs), SNARE-associated molecules, and sorting receptors involved in endosomal-lysosomal trafficking (Figure 3A). The only exception was the vesicle (v)-SNARE molecule VAMP7, which was upregulated about 2-fold in *Sort1*$^{-/-}$ CTLs (Figure 3B). A colocalization of Sortilin and VAMP7 could not be visualized (Figure S2C). Treatment with lysosomal protease inhibitors and cycloheximide increased VAMP7 protein expression in WT CTLs but not in *Sort1*$^{-/-}$ CTLs (Figure 3C). We conclude that Sortilin could be involved in the trafficking and recycling of VAMP7 to or from a degradative compartment.

VAMP7 interacts with the δ subunit of adaptor protein complex-3 (AP-3), and AP-3-depleted cells aberrantly sort CD63 to the plasma membrane (Clark et al., 2003; Dell'Angelica et al., 1999). We confirmed that CD63 cell surface localization was decreased in VAMP7-overexpressing *Sort1*$^{-/-}$ CTLs compared with WT CTLs (Figure 3D). Furthermore, through siRNA-mediated donwregulation of VAMP7, the release of granzyme A but not β-hexosaminidase from CTLs was consistently decreased (Figures 3E and 3F). Applying subcellular fractionation and immunoblot analysis, no gross alteration in VAMP7 distribution or any other organelle markers was obtained (Figure S2D). Trafficking of newly synthesized granzyme B in *Sort1*$^{+/+}$ and *Sort1*$^{-/-}$ CTLs was indiscriminable, as shown by the fact that in a pulse-chase experiment occurrence of the endoglycosidase-H (EndoH)-resistant form, indicative of a proper transit from the ER to the medial Golgi, was seen in both genotypes after 20 min (Figure S2E).

To resolve the kinetics of granzyme redistribution, we incubated *Sort1*$^{+/+}$ and *Sort1*$^{-/-}$ CTLs at 19.5°C to accumulate granzymes in the Golgi and then shifted the temperature to 37°C

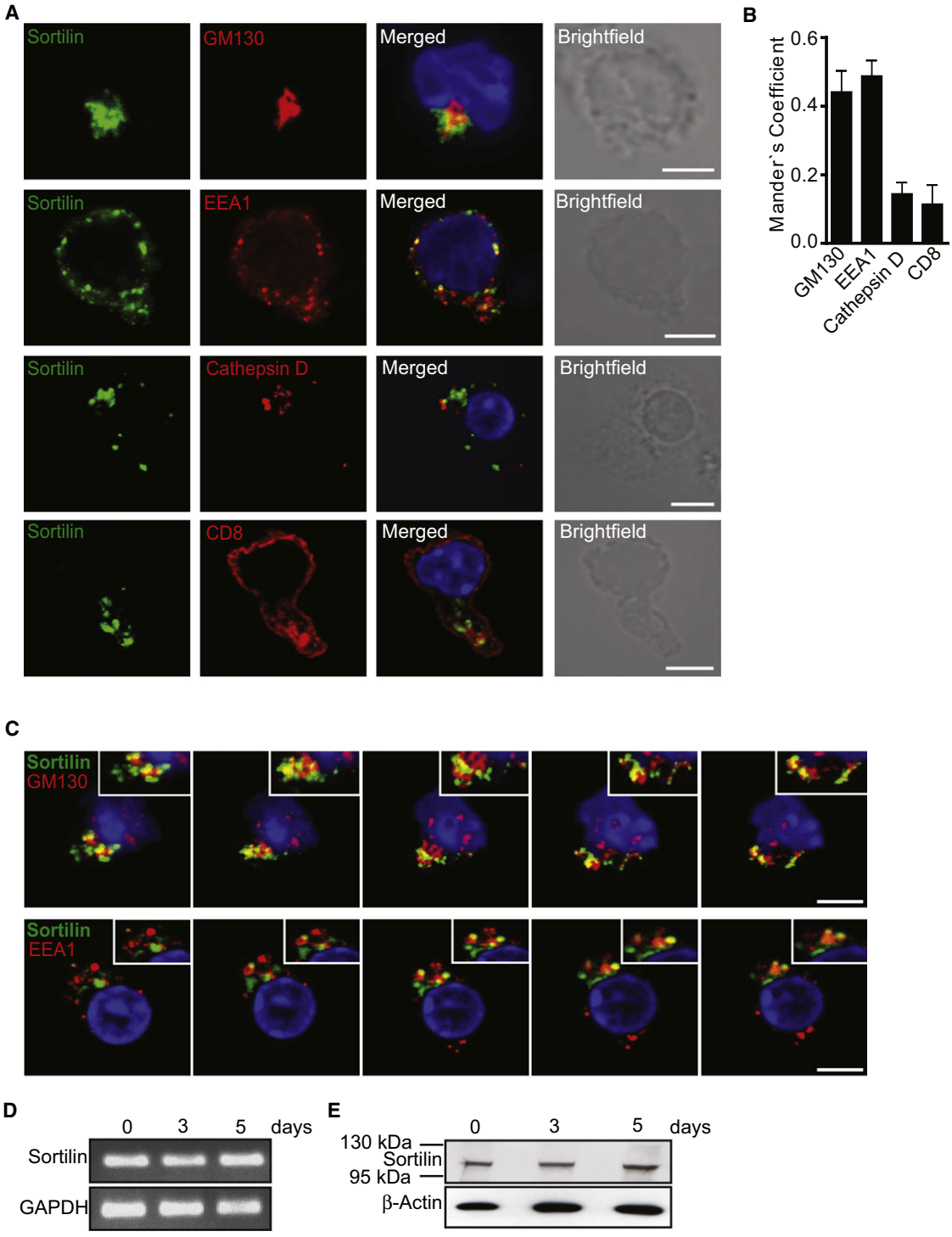

Figure 1. Localization of Sortilin in T Cells

(A) CTLs from C57BL/6 WT mice (n = 5–6) were stimulated with anti-CD3 and CD28, followed by $CD8^+$ purification, and transfected with GFP-tagged full-length Sortilin (day 4). Cells were grown on coverslips and stained with anti-GM130, EEA1, cathepsin D, and CD8; blue, DAPI stain. Analysis was done by confocal microscopy; images show medial confocal optical sections. Scale bars represent 5 μm.

(B) Quantitative analysis of Sortilin-GFP structures overlapping with the indicated organelle-specific markers. Bars show the Mander's coefficient indicating a colocalization between Sortilin-GFP and the organelle marker. Data represent the mean ± SEM. Two independent experiments with at least 10–30 cells for each marker protein were evaluated.

(C) Representative planes of a z series of confocal optical sections are shown for the markers with the highest colocalization coefficients. Images were taken at an increment of 0.6 μm. Insets are 2- to 3-fold magnification of the overlap area. Scale bars represent 5 μm.

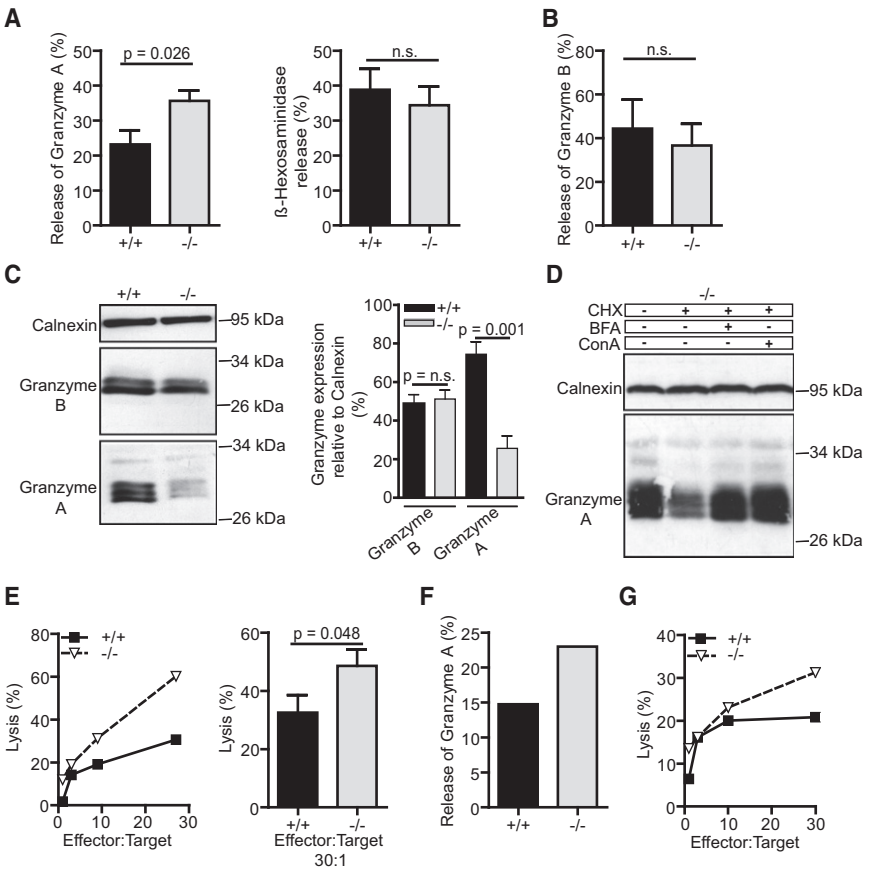

Figure 2. Sortilin Deficiency Leads to an Enhanced Release of Granzyme A and Increased Allogeneic Cytotoxicity

(A and B) CTLs from BALB/c (WT, +/+) and *Sort1*$^{-/-}$ (−/−) mice were generated through anti-CD3 CD28 stimulation and used at days 5–6. Secretion of effector molecules was induced with anti-CD3 CD28. After 4 hr, cell supernatant was analyzed for granzyme A and β-hexosaminidase activity (A). Granzyme B (B) content was analyzed by ELISA. Bars show the mean ± SEM of seven (A) and four (B) independent experiments. In each experiment, pooled cells from three mice per group were used.

(C) Equal amounts of *Sort1*$^{+/+}$ and *Sort1*$^{-/-}$ (C57BL/6) CTL lysates were analyzed by immunoblotting for granzyme A and B expression; calnexin served as loading control. Antigen expression was quantified by densitometric scanning. Granzyme expression was first calculated relative to calnexin content and then these ratios were compared between WT and *Sort1*$^{-/-}$ CTLs and expressed in percent. Bars show the mean ± SD of seven independent experiments; CTLs were pooled from at least two to three mice per group in each experiment.

(A–C) p values were determined by Mann-Whitney test; n.s., nonsignificant.

(D) *Sort1*$^{-/-}$ CTLs were treated with or without cycloheximide (CHX, 40 μg/ml), brefeldin A (BFA, 5 μg/ml), or concanamycin A (Con A, 0.5 μM) for 4 hr. Lysates were analyzed by immunoblotting with anti-granzyme A and anti-calnexin. One representative experiment of three experiments performed with two animals per genotype in each experiment.

(E) Cytolytic activity of MLR-derived CTLs (BALB/c, H-2^{d}) against allogeneic MCA205 target cells (H-2^{b}). One representative example of five independent experiments is shown with pooled effector cells from three mice per group. Data represent mean values ± SEM of experiments performed in triplicate. On the right, statistical presentation of cytolytic killing at the effector to target ratio 30:1. p values were determined by one-tailed Mann-Whitney test.

(F) NK cells (day 9) were generated from WT (C57BL/6) and *Sort1*$^{-/-}$ mice. Release of granzyme A from NK cells was effectuated with PMA and ionomycin. Bars show the mean of two independent experiments; NK cells were pooled from three mice per group in each experiment.

(G) Cytolytic activity of purified NK cells (C57BL/6, H-2^{b}) against allogeneic YAC-1 target cells (H-2^{d}). One representative example of two experiments is shown with pooled effector cells from three mice per group. Data represent mean values of experiments performed in triplicate.

See also Figure S1.

to resume their anterograde transport (Figures 3G and 3H). At 0 min, a strong colocalization of granzyme A and granzyme B in a perinuclear Golgi-like region indicated that both granzymes accumulated in the Golgi because of low temperature arrest. After 10 and 45 min, a clear vesicular staining pattern revealed that both granzymes had passed the Golgi. In WT CTLs, granzyme A exhibited considerable colocalization with granzyme B-positive carriers, suggesting that both granzymes were transported via the same route. In contrast, granzyme A localization in *Sort1*$^{-/-}$ CTLs clearly deviated from this pattern, indicating that Sortilin affected the intracellular redistribution toward a post-Golgi compartment. Additionally, we excluded the possibility that endocytic uptake and recycling of transferrin were influenced by Sortilin (data not shown). In summary, decreased VAMP7 lysosomal degradation in *Sortilin*$^{-/-}$ CTLs was associated with decreased CD63 surface expression and enhanced granzyme A release.

Strong Reduction of IFN-γ Secretion in *Sort1*$^{-/-}$ Mice

Secretion of the effector cytokines IFN-γ and TNF-α is putatively dependent on the constitutive secretory pathway. Upon TCR activation, IFN-γ secretion was drastically diminished in *Sort1*$^{-/-}$ compared to *Sort1*$^{+/+}$ CTLs (Figure 4A). In keeping with the data from CTLs, Th1 (>2-fold) and NK (2-fold) cells from *Sort1*$^{-/-}$ mice also exhibited greatly reduced IFN-γ secretion (Figures 4B and 4C). In contrast, in CTLs and Th1 cells derived from *Sort1*$^{+/+}$ and *Sort1*$^{-/-}$ mice, we could not detect a difference for TNF-α (Figures S3A and S3B).

(D) Quantitative RT-PCR analysis of Sortilin mRNA expression relative to GAPDH in murine naive CD8^{+} T cells (day 0) and activated CTLs derived from an anti-CD3 and CD28 stimulation (day 3 and 5). Results are representative of two independent experiments, with pooled CTLs from four mice for each group.

(E) Purified CTLs were used unstimulated (day 0) or stimulated (day 3 and 5). Cell lysates were analyzed by immunoblotting for Sortilin; β-actin was used as a loading control. One representative example of at least three experiments is shown.

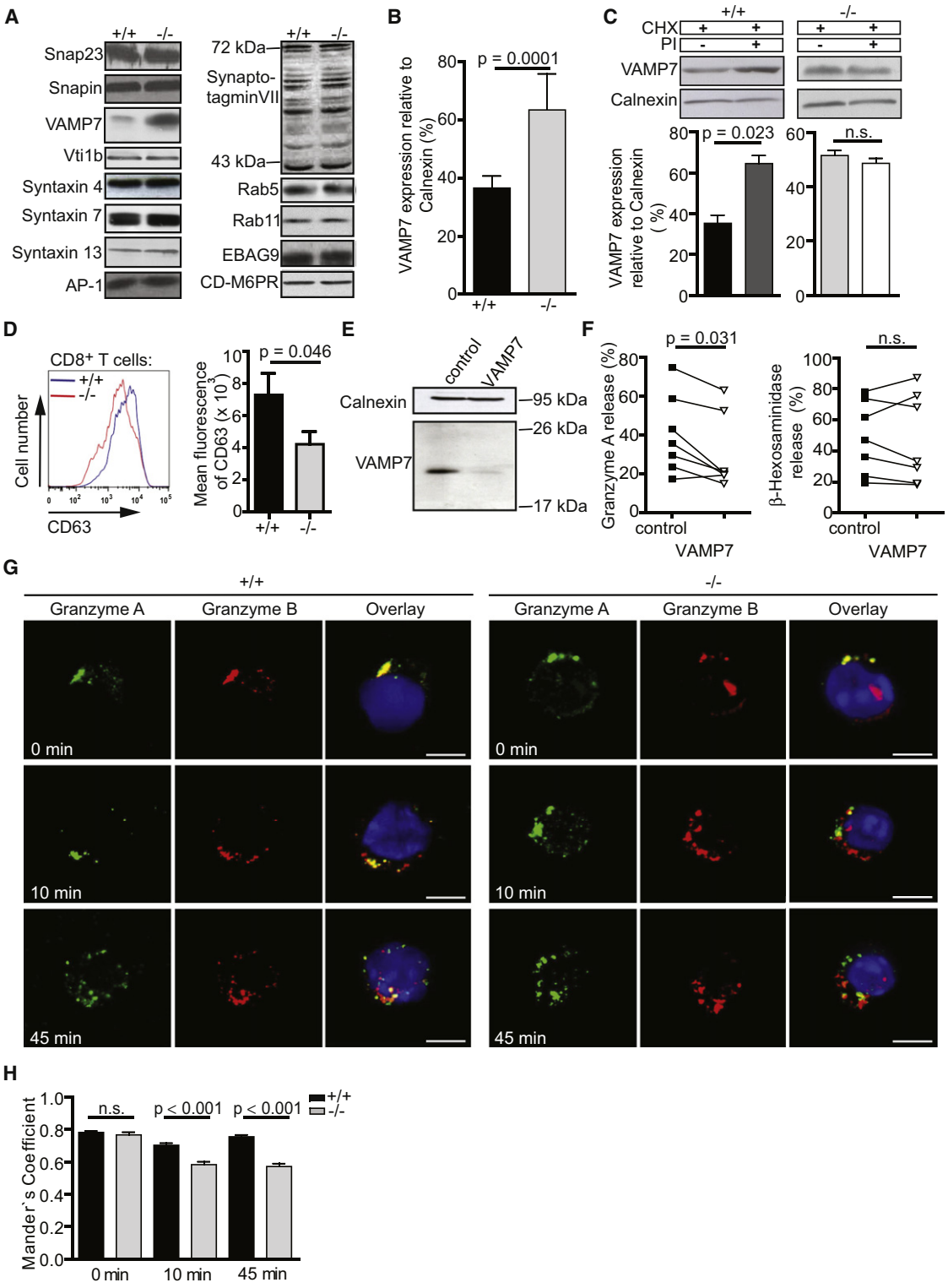

Figure 3. Sortilin Deficiency Results in a Compensatory Increase of VAMP7 Expression

(A) Equal amounts of *Sort1*$^{+/+}$ (C57BL/6) and *Sort1*$^{-/-}$ CTL lysates, generated from anti-CD3 CD28-stimulated T cells, were analyzed by immunoblotting for the proteins indicated. SynaptotagminVII occurred in several splice variants. One representative example of at least three experiments is shown.

(B) Antigen expression was quantified by densitometric scanning. VAMP7 expression was first calculated relative to calnexin content and then these ratios were compared between WT and *Sort1*$^{-/-}$ CTLs and expressed in percent. Bars show the expression of VAMP7 ± SD of nine experiments.

(C) CTLs from WT or *Sort1*$^{-/-}$ mice were cultured on day 6 for 12 hr in the presence or absence (+/−) of cycloheximide (CHX, 40 μg/ml) and the lysosomal protease (PI) inhibitors E-64 (10 μg/ml) and leupeptin (1 mg/ml). Medium with inhibitors was exchanged after 6 hr. Protein lysates were analyzed by immunoblotting with

Pulse-labeled CTLs were incubated on uncoated or anti-CD3-precoated plates to distinguish constitutive and inducible release (Rüder et al., 2009). Constitutive and induced discharge of labeled proteins showed no difference between WT and *Sort1*$^{-/-}$ CTLs (Figure S3C). We conclude that Sortilin affects the intracellular transit time of only a discrete set of secretory proteins.

To study the immunological consequences of Sortilin deletion, mice were challenged with adenoviruses at sublethal dosages. On day 6 after infection, the serum concentration of IFN-γ was reduced by one-half in *Sort1*$^{-/-}$ mice compared with WT mice (Figure 4D). Reduction of serum IFN-γ was not due to lower T cell activation status in *Sort1*$^{-/-}$ animals, as shown by the fact that IL-2 serum concentration was similar compared with WT controls (Figure S3D). Likewise, frequencies of CD4$^+$IFN-γ$^+$ and CD8$^+$IFN-γ$^+$ effector T cells from infected mice were comparable in both genotypes (Figure 4E). Clearance of adenovirus-infected hepatocytes requires IFN-γ activity. Corresponding to decreased circulating IFN-γ serum concentrations, at day 6 after adenovirus infection the activities of hepatic transaminases alanine aminotransferase (ALT) and aspartate aminotransferase (AST) in *Sort1*$^{-/-}$ mice were considerably higher (Figure 4F). In accordance, when *Sort1*$^{+/+}$ and *Sort1*$^{-/-}$ mice were challenged with *L. monocytogenes* at sublethal dosages, substantially enhanced concentrations of IFN-γ in WT serum were measured on day 2 and 6 (Figures 4G and 4H). Circulating serum IL-2 was similar in *Sort1*$^{+/+}$ and *Sort1*$^{-/-}$ mice (Figure S3E), likewise peptide-specific restimulation of splenocytes demonstrated indistinguishable frequencies of CD8$^+$IFN-γ$^+$ effector T cells in both genotypes at days 6 (Figure 4I) and 8 (data not shown). Uninfected *Sort1*$^{+/+}$ and *Sort1*$^{-/-}$ mice harbored comparable amounts of serum IFN-γ (Figures S3F and S3G). Gene-deleted animals were compromised in their T cell-mediated clearance function, as shown by the fact that *L. monocytogenes*-infected *Sort1*$^{-/-}$ mice exhibited substantially higher bacterial titers (day 5) in spleen compared with WT mice (Figure 4J). In an in vivo killing assay against listeriolysin O (LLO)-peptide loaded splenocytes, *Sort1*$^{+/+}$ and *Sort1*$^{-/-}$ mice infected with *L. monocytogenes* exhibited a comparable cytolytic activity (Figure S4H).

The priming capacity of bone marrow-derived dendritic cells (DCs) was compared with ovalbumin (OVA)-specific CD8$^+$ T cells from OT-I and CD4$^+$ T cells from OT-II mice as responders. OVA-pulsed DC stimulators from *Sort1*$^{+/+}$ and *Sort1*$^{-/-}$ animals exhibited comparable stimulatory capacity for CD8$^+$ and CD4$^+$ T cells (data not shown).

Whereas the adenovirus infection model was evaluated at day 6, when CTLs experienced a peak in granzyme A gene expression (Figure S3I), serum from *L. monocytogenes*-infected mice was also obtained on day 2 after infection. Thus, differences at day 2 are probably attributable to IFN-γ release from effector cells other than conventionally primed αβ T cells, such as γδ T cells, NK T cells, or possibly NK cells instead (Andersson et al., 1998; Stetson et al., 2003). Peak IFN-γ gene expression was obtained at day 3 (Figure S3J). In summary, decreased release of IFN-γ in *Sort1*$^{-/-}$ mice was not due to different effector cell numbers, activation status, or synthesis rate.

Attenuation of Inflammatory Bowel Disease in *Rag2*$^{-/-}$ Mice Transplanted with *Sort1*$^{-/-}$ CD4$^+$CD25$^{lo/-}$ T Cells

Immunodeficient *Rag2*$^{-/-}$ mice were adoptively transferred with sorted CD4$^+$CD25$^{lo/-}$ T cells from WT and *Sort1*$^{-/-}$ mice (Figures S4A and S4B). Transfer of regulatory T cell-deficient CD4$^+$ T cell populations into *Rag2*$^{-/-}$ mice induces inflammatory bowel disease (IBD), a condition in which IFN-γ plays a leading role (Ito and Fathman, 1997; Schneider et al., 2007). *Rag2*$^{-/-}$ mice that received WT T cells demonstrated an accelerated loss of body weight (20%) within the 3 week observation period (Figure 5A). In the same time interval, *Rag2*$^{-/-}$ mice reconstituted with *Sort1*$^{-/-}$ T cells lost only 5% of their initial body weight. Circulating serum IFN-γ was only 40% in *Sort1*$^{-/-}$ T cell recipients compared to WT (Figure 5B). Histologic scoring of descending colonic tissue specimens showed an altered frequency distribution of severe colitis pathology (Figure S4C). Corresponding with higher serum IFN-γ concentrations, disease scores >2 were more frequent in *Sort1*$^{+/+}$ CD4$^+$ T cell *Rag2*$^{-/-}$ recipients (Figure 5C). CD3$^+$ T cell infiltrates within mucosa and submucosa in both groups were clearly detectable (Figure S4C). We conclude that lack of Sortilin can partially protect from severe tissue damage resulting from reduced IFN-γ release.

In the Absence of Sortilin, IFN-γ Is Retained in the Golgi Complex

To investigate where the transport of IFN-γ in CTLs and Th1 cells in the absence of Sortilin might be compromised, we examined IFN-γ localization in CTLs. IFN-γ and GM130 colocalization in both genotypes under resting conditions revealed considerable

anti-VAMP7. Representative examples out of three experiments performed are shown. VAMP7 and calnexin expression of all three experiments was quantified by densitometric scanning and expressed as in (B); the ratios were compared between the different treatment groups.

(D) CTLs were stimulated for 4 hr with anti-CD3 CD28. Viable CD8-positive cells were gated for analysis of CD63 fluorescence intensity by flow cytometry. One representative example is shown. Bars show the mean values ± SEM for the geo mean fluorescence intensity (MFI) of CD63 cell surface expression on *Sort1*$^{+/+}$ and *Sort1*$^{-/-}$ CTLs; n = 8 for WT and n = 9 independent measurements for *Sort1*$^{-/-}$.

(B–D) p value was determined by Mann-Whitney test.

(E) *Sort1*$^{+/+}$ CTLs were transfected with siRNA specific for VAMP7 or a scrambled siRNA as a negative control. After 24 hr, VAMP7 and calnexin expression was analyzed by immunoblotting. One representative example out of seven experiments performed is shown.

(F) Each data point represents data of one independent experiment. Secretion of effector molecules was induced with anti-CD3 CD28. After 4 hr, cell supernatant was analyzed for granzyme A and β-hexosaminidase activity. p values were determined by Wilcoxon signed rank test; n.s., nonsignificant.

(G) CTLs were transfected with granzyme A-Myc-Flag. CTLs were first incubated at 19.5°C and then shifted to 37°C for 10 and 45 min. Cells were then stained as indicated in Figure 1A. Images are presented as medial confocal optical sections. For each time point and genotype, statistical analysis of the Mander's coefficient was performed on 6–10 optical sections for at least 10 cells. These contiguous optical planes contained all the three-dimensional fluorescence information. Scale bars represent 5 μm.

(H) Quantitative and time-resolved intracellular redistribution of granzyme A and B. Bars show the degree of colocalization of granzyme A and B, as determined by Mander's coefficient for each optical section of a z stack. Data are means ± SEM of two independent experiments. p value was determined by Student's t test.

In all panels, pooled CTLs from at least two to three mice per group in each experiment were used. See also Figure S2.

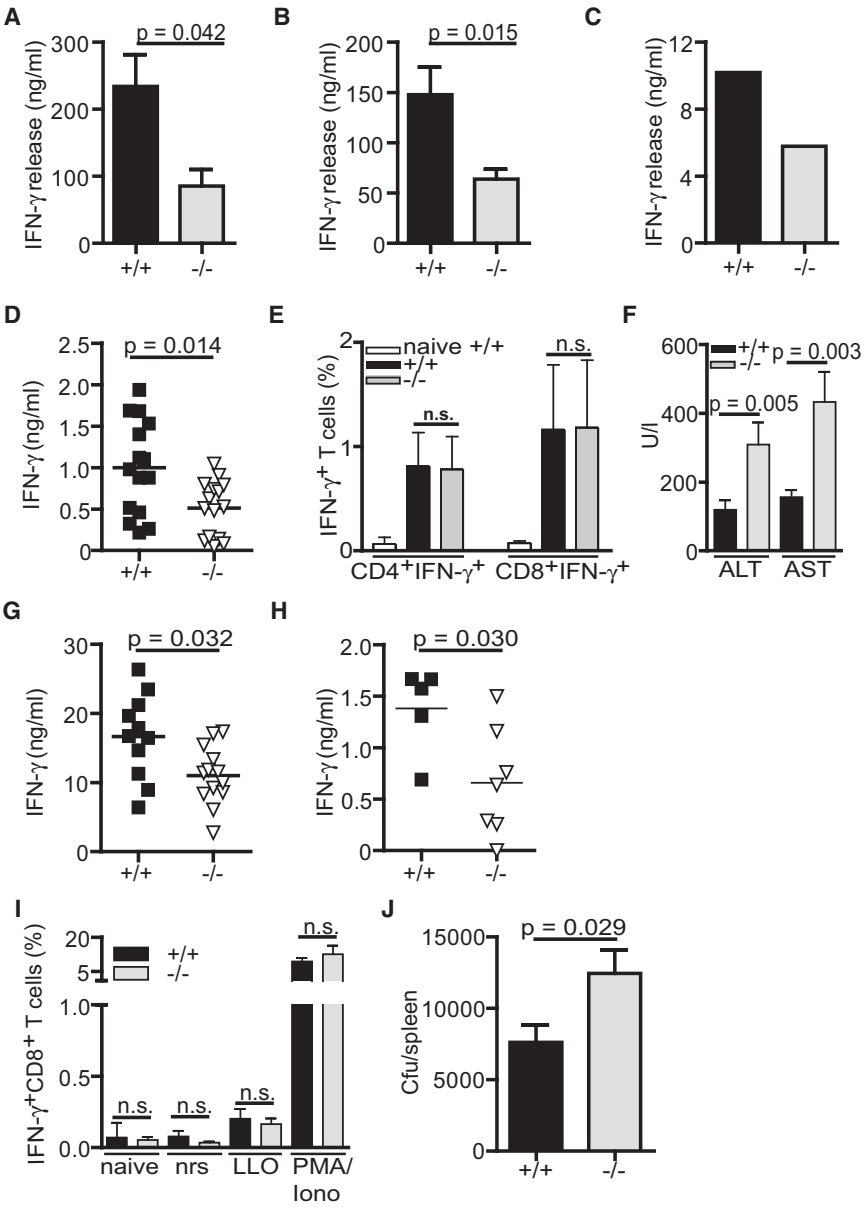

Figure 4. Reduced Secretion of IFN-γ in Sortilin-Deficient Mice

(A) CTLs from *Sort1*$^{+/+}$ (BALB/c) and *Sort1*$^{-/-}$ mice were generated through anti-CD3 CD28 stimulation and used at days 5–6. Secretion of IFN-γ was induced with anti-CD3 CD28.

(B) In vitro differentiated Th1 cells were induced to release IFN-γ as in (A).

(C) NK cells (day 9) were generated from WT (C57BL/6) and *Sort1*$^{-/-}$ mice. Release of IFN-γ from NK cells was effectuated with PMA and ionomycin. After 4 hr, secretion was determined by ELISA.

Bars show the mean ± SD of nine (A, B) and two (C) independent experiments; CTLs, Th1, and NK cells were pooled from at least two to three mice per group in each experiment.

(D) *Sort1*$^{+/+}$ (C57BL/6) and *Sort1*$^{-/-}$ mice were challenged by injection (i.v.) of 1 × 10^8 PFU adenovirus. On day 5 after challenge, IFN-γ in vivo capture antibody was injected (i.p.). After 20 hr, secretion of IFN-γ in the serum was analyzed by in vivo capture assay. Three independent experiments with 15 mice for each group were performed.

(E) Splenocytes from adenovirus-infected mice were restimulated overnight with adenovirus-transduced WT DCs. For the final 4 hr of stimulation, BFA was included. Splenocytes were stained with anti-CD4 or CD8, followed by intracellular anti-IFN-γ detection and flow cytometry analysis. Bars indicate the mean percentage of IFN-γ$^+$ cells among the CD8$^+$ or CD4$^+$ T cells, ±SD of three independent experiments with n = 10 mice for each genotype and n = 3 naive mice.

(F) Bars indicate mean values ± SD and show the enzymatic activity of the transaminases ALT and AST in serum. Shown are data of two independent experiments performed with at least n = 7 mice per group.

(G) *Sort1*$^{+/+}$ (BALB/c) and *Sort1*$^{-/-}$ mice were infected with 5 × 10^3 *L. monocytogenes* (i.v.).

(G and H) After 2 (G) and 6 (H) days, mice were sacrificed and serum levels of IFN-γ were analyzed by ELISA. Shown are data of two independent experiments analyzed at day 2 (left) and day 6 (right).

(I) Bars indicate mean values ± SD and show the frequencies of IFN-γ$^+$ cells among the CD8$^+$ splenocytes 6 days after infection with *L. monocytogenes* and an additional restimulation for 4 hr with LLO-peptide or with PMA and ionomycin. Nrs, splenocytes from infected mice, not restimulated. Shown are data of one experiment with n = 5 (WT), 7 (*Sort1*$^{-/-}$), and 3 (naive) mice analyzed. n.s., nonsignificant.

(J) *Sort1*$^{+/+}$ (BALB/c) and *Sort1*$^{-/-}$ mice were infected with 5 × 10^3 *L. monocytogenes* (i.v.). On day 5, mice were sacrificed and bacterial titers in spleen (colony forming units, cfu) were determined. Results represent the mean ± SD of n = 12 WT and n = 14 *Sort*$^{-/-}$ mice per group.

All p values were determined by Mann-Whitney test; n.s., nonsignificant. See also Figure S3.

accumulation of IFN-γ at the Golgi complex in *Sort1*$^{-/-}$ CTLs, whereas in WT CTLs IFN-γ was more dispersed in a cytoplasmic granular pattern (Figure 6A; Movies S1 and S2). Quantitation of the ratios between IFN-γ fluorescence in the Golgi versus whole cell-localized fluorescence indicated that values for CTLs and Th1 cells were increased, respectively, by 1.6-fold and 1.92-fold in *Sort1*$^{-/-}$ cells compared with *Sort1*$^{+/+}$ cells (Figures 6B, S5A, and S5B).

To resolve the kinetics of IFN-γ transport from the Golgi complex to the plasma membrane, we performed a temperature block and shift experiment. In WT CTLs, only minor colocalization of IFN-γ and GM130 persisted after 5 min, indicating that IFN-γ had passed the Golgi (Figures 6C and 6D). Accordingly, immunofluorescence intensity of IFN-γ in the Golgi region versus the whole cell as a measure for transport kinetics decreased over time (Figure 6D). In contrast, in *Sort1*$^{-/-}$ CTLs high colocalization values of IFN-γ and GM130 were obtained after 5 min, and these values persisted 30 min after the temperature shift. Specific interaction between Sortilin and IFN-γ was confirmed with coimmunoprecipitation experiments in transfected HEK293 cells (Figure 6E), as well as by confocal microscopy (Figures S5C and S5D). Most of this activity showed additional strong overlap

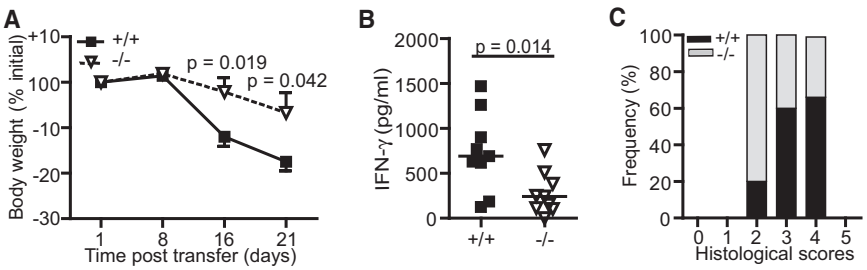

Figure 5. Loss of Sortilin Mitigates Chronic Colitis in the CD4$^+$CD25$^{lo/-}$ Transfer Model

(A) Sorted CD4$^+$CD25$^{lo/-}$ T cells from WT (C57BL/6) or *Sort1*$^{-/-}$ mice were adoptively transferred into *Rag2*$^{-/-}$ mice. Graph represents weight loss in percent, expressed as mean values ± SEM of two independent experiments with n = 9 mice per genotype.

(B) Secretion of IFN-γ into serum was measured at day 21, when animals were sacrificed.

(A and B) Bars show mean values; p values as determined by Student's t test.

(C) Frequency distribution of histological disease scores were calculated based on the examination of H&E stainings of descending colon specimen. Histologies were graded from 0 (unaffected) to 5 (most severe colitis).

See also Figure S4.

with GM130, indicating that Sortilin acts as a sorting receptor for IFN-γ at the TGN.

Intracellular Trafficking of IFN-γ in CTLs

To track the trafficking route of IFN-γ in WT CTLs beyond its passage through the Golgi, kinetics of transferrin routing upon endocytosis and recycling were examined. Extensive colocalization between IFN-γ, transferrin, and the early endosome marker EEA1 was observed beginning at 10 min and was stronger at 20 min (Figures 7A and 7B). At 45 min, these structures were clearly separated, indicating that IFN-γ and transferrin employed distinct routes before their release at the plasma membrane. Previously, costaining of IFN-γ with Rab19$^+$ vesicles at the IS in Th1 cells has been demonstrated (Huse et al., 2006), but a function for this Rab19$^+$ carrier population is unknown. We also observed transient IFN-γ colocalization with Rab19$^+$ organelles, with 20 min delay (Figures 7A and 7B). Rab19$^+$ and IFN-γ$^+$ structures were separated at 45 min. Overlap between Rab19$^+$ vesicles and the recycling endosome marker Rab11 was not observed (data not shown). Colocalization of endogenous IFN-γ with Rab3d$^+$ secretory granules did not occur (Figures 7A and 7B). We conclude that Sortilin controls the transport of IFN-γ from the Golgi toward the endosomes, where the cytokine route intersects with endocytosed transferrin and Rab19$^+$ vesicles. However, presuming that transferrin after its transit through early endosomes subsequently enters a recycling endosome compartment, we excluded that IFN-γ entered such vesicles for release. Although colocalization with IS-proximal Golgi complexes was obtained, IFN-γ lacked colocalization with the lytic granule markers cathepsin D or Rab27a (Figures 7C and 7D; data shown for cathepsin D). In summary, we suggest that under physiologic conditions, secretion of IFN-γ occurs on an alternative exocytic route, distinct from recycling endosomes and secretory lysosomes.

DISCUSSION

In this study we demonstrate that Sortilin plays a pivotal role in the regulation of the adaptive immune response through control of two separate trafficking pathways in effector T cells and NK cells. Sortilin loss conferred CTLs and NK cells with an enhanced capacity for granzyme A release and improved allogeneic cytotoxicity in vitro. We suggest that compensatory upregulation of the SNARE molecule VAMP7 in *Sort1*$^{-/-}$ CTLs could account for this effect. VAMP7, in conjunction with the counterstructure-SNAREs syntaxin 7, syntaxin 8, and vti1b, is required for both homotypic late endosome fusion and heterotypic fusion with lysosomes (Antonin et al., 2000; Pryor et al., 2004). In agreement with our observation on CTLs, a role for VAMP7 in target cell killing has been obtained in human NK cells, where siRNA-mediated downregulation inhibits cytolytic activity (Krzewski et al., 2011; Marcet-Palacios et al., 2008). Increased amounts of VAMP7 in the absence of Sortilin is probably caused by protection from proteolytic degradation, as shown by the effect of lysosomal protease inhibitors. In accordance neuronal BDNF amounts are also modulated by Sortilin-dependent lysosomal degradation (Evans et al., 2011).

Increased VAMP7 amounts could enhance the efficacy of vesicle fusion, thereby improving granzyme delivery at the late endosome to secretory lysosome trafficking step. VAMP7 interferes with an AP-3-dependent trafficking step from endosomes toward the lysosomal compartment; in mice that lack a functional AP-3 complex, CD63 is missorted toward the plasma membrane (Clark et al., 2003; Rous et al., 2002). Reduced plasma membrane delivery of CD63 and enhanced granzyme A release from lytic granules would be consistent with a regulatory role of Sortilin in these processes. Although Sortilin is unlikely to interact with the membrane-bound molecule VAMP7 directly, we envisage that Sortilin mediates instead transport of lysosomal enzymes to the site of VAMP7 degradation.

Differential release of granzyme A and B in a Sortilin-dependent manner could relate to their complex posttranslational modifications (Russell and Ley, 2002; Trapani, 2001). The proapoptotic effects of both granzymes in target cells are nonredundant, and it remained puzzling how the differential timing of cell death induction through either granzyme A or B is regulated. Enhanced provision of an enzymatic active granzyme A form in the supernatant of *Sort1*$^{-/-}$ CTLs could be in agreement with the existence of specialized lysosomal compartments, lysosomal maturation stages, or trafficking routes, respectively, that deliver the cytolytic agents at different speed (Russell and Ley, 2002). We note that in the absence of Sortilin, granzyme A trafficking deviated from the granzyme B routing, and furthermore the molecule was lost rapidly from intracellular stores; this process was sensitive to post-Golgi transport or lysosomal proteolysis inhibition.

In the absence of Sortilin, IFN-γ release was drastically diminished. CTLs, Th1 cells, and NK cells share the basic exocytosis machinery necessary to secrete common immunologic modulators (Rüder et al., 2009; Stinchcombe et al., 2004). The

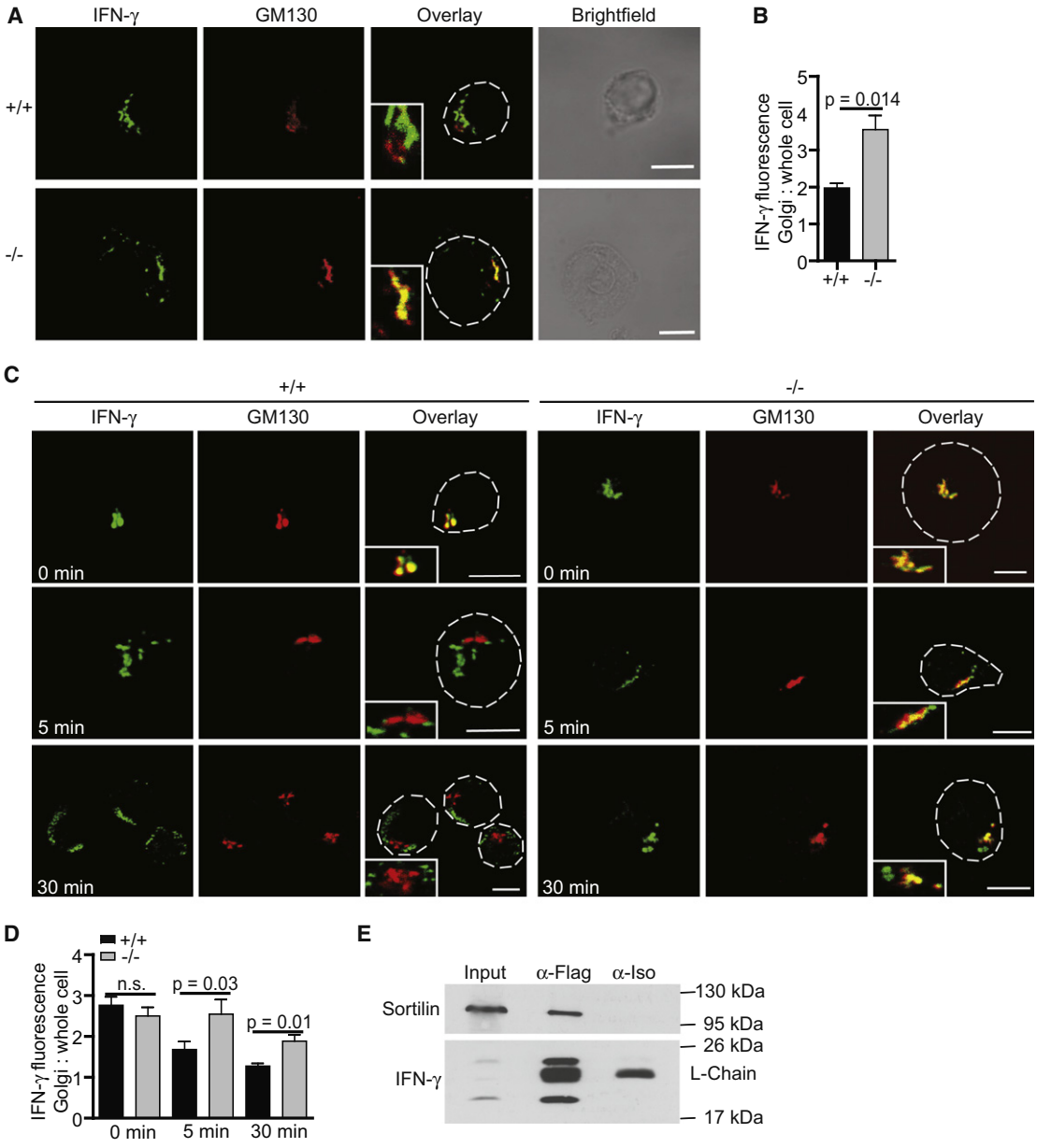

Figure 6. Exit of IFN-γ from the Golgi Is Severely Delayed in *Sort1*$^{-/-}$ CTLs

(A) CTLs from *Sort1*$^{+/+}$ (C57BL/6) and *Sort1*$^{-/-}$ (day 5) mice were stained with the antibodies indicated, followed by confocal microscopy analysis. Insets are 2- to 3-fold magnification of the Golgi zone.

(B) Bars show the ratio of Golgi-associated versus total cell-associated IFN-γ fluorescence, as defined by GM130 positivity. Data are means ± SEM of three independent experiments with n = 21 cells (*Sort1*$^{+/+}$) and 35 cells (*Sort1*$^{-/-}$) evaluated.

(C) CTLs were first incubated at 19.5°C, and then shifted to 37°C for up to 30 min. Cells were treated and stained as indicated in (A). Insets are 2- to 3-fold magnification of the Golgi zone.

(A and C) Dashed white lines indicate cell boundaries; medial confocal optical sections are shown. Scale bars represent 5 μm.

(D) Quantitative and time-resolved evaluation of IFN-γ exit from the Golgi complex. Bars show the ratio of Golgi-associated versus total cell-associated IFN-γ fluorescence at the indicated time points. Data are means ± SEM of three independent experiments with at least ten cells for each time point per group.

(B and D) p values were determined by Mann-Whitney test; n.s., nonsignificant.

(A–D) Cells were derived from at least eight mice per genotype.

(E) HEK293A cells were transiently transfected with Sortilin-Myc and IFN-γ-Flag-Myc, then lysed and subjected to immunoprecipitation with anti-Flag-M2. Coimmunoprecipitated Sortilin-Myc was detected by immunoblotting with anti-Myc. IFN-γ-Flag-Myc was detected with anti-Flag-M2. Input was 1/20 volume of the reaction mixture. L-chain, antibody light chain. One representative experiment out of three performed.

See also Figure S5 and Movies S1 and S2.

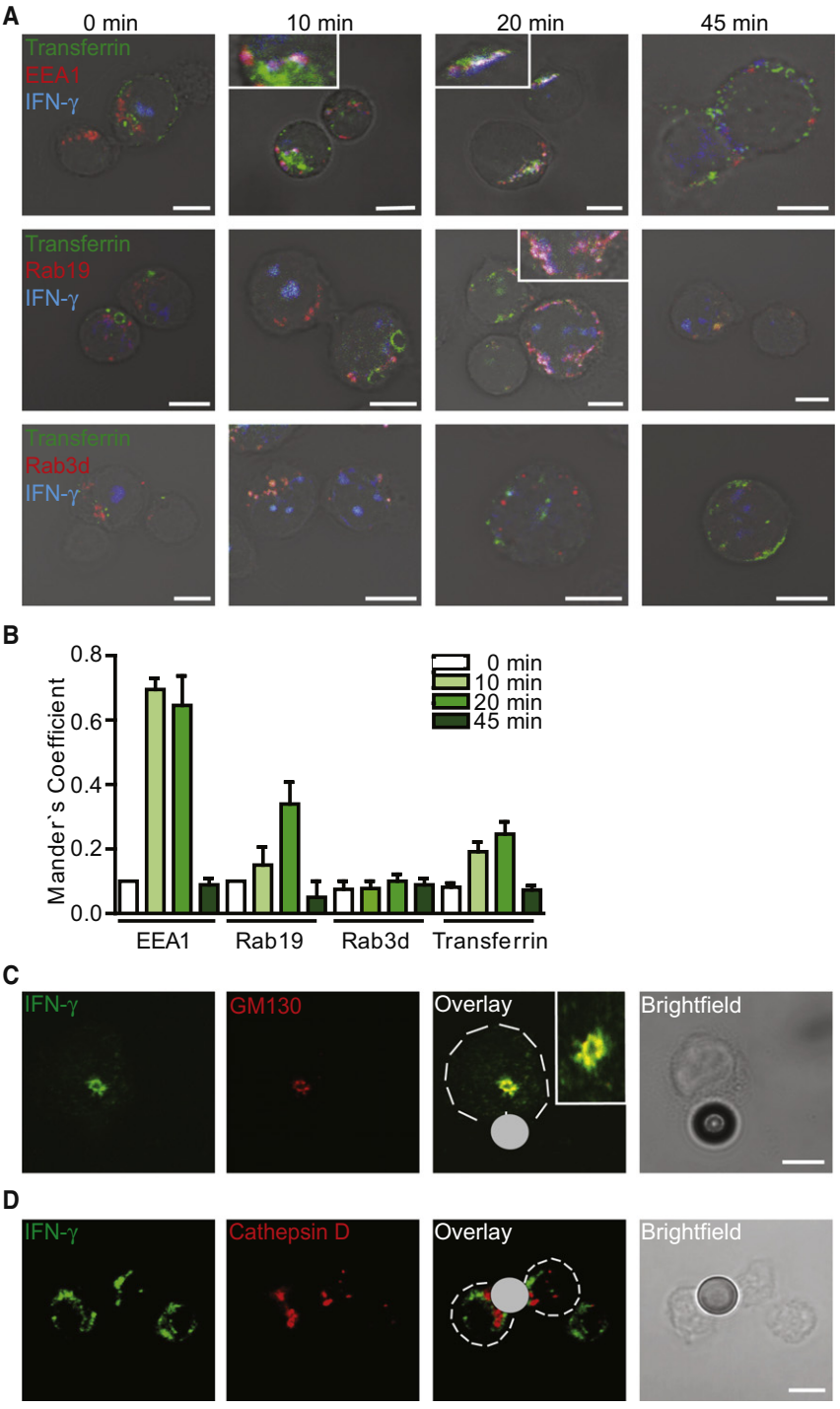

Figure 7. IFN-γ Is Released Separately from Recycling Endosomes

(A) CTLs from C57BL/6 WT mice (day 5–6) were incubated with Alexa Fluor-488-labeled transferrin for 30 min. The recycling phase was induced by washing the cells, followed by competition with excessive unlabeled transferrin. Cells were seeded on coverslips, precoated with anti-CD3 CD28 for 15 min at 4°C, followed by a chase at 37°C for the times indicated. Cells were stained with the indicated antibodies and analyzed by confocal microscopy. Medial confocal optical sections are shown, with one representative example of at least two experiments performed per staining. Cells were derived from at least six to eight mice per genotype. Insets are 2- to 3-fold magnifications of the fusion zone between transferrin and organelle markers. Scale bars represent 5 μm.

(B) Quantitative analysis of IFN-γ structures overlapping with endocytosed transferrin and the indicated organelle-specific markers. Bars show Mander's coefficient at the indicated time points. Data are means ± SD of at least two independent experiments with n = 10 cells for each time point per staining.

(C and D) CTLs from WT mice were mixed with CD3 CD28 T cell expander beads. Conjugates were then plated on coverslips for 30 min at 37°C, fixed, and stained with the antibodies indicated. One representative example of at least two experiments with n = 10 cells per staining is shown. Dashed white lines indicate cell boundaries, and beads are pseudocolored in white (overlay). Scale bars represent 5 μm.

adenovirus infection model proved that loss of Sortilin reduces the physiologic clearance capacity, as indicated by the elevation of liver enzymes. Destruction of adenovirus-transduced hepatocytes is usually attributed to the cytolytic activity of $CD8^+$ T cells (Yang et al., 1994), but IFN-γ also decreases adenoviral transgene expression (Sung et al., 2001). Enhanced liver damage in *Sort1*$^{-/-}$ mice would be consistent with a leading role of defective IFN-γ secretion. In line with this interpretation, clearance of *L. monocytogenes* from spleen was also impaired in *Sort1*$^{-/-}$ mice. For the effector phase after in vivo challenge, we have to consider two effects in the opposing direction: a putatively protective effect resulting from enhanced granzyme A release and an immune response dampening effect through IFN-γ reduction. Consistent with our in vivo data, it has been demonstrated that mice deficient for the IFN-γ receptor have an increased susceptibility for *L. monocytogenes* and vaccinia virus infections (Huang et al., 1993). On the other hand, granzyme A-deficient mice are shown to efficiently control LCMV and *L. monocytogenes* infections (Ebnet et al., 1995). More recently, it was found that granzyme-deficient mice harbor even lower *L. monocytogenes* titers and decrease splenic pathology upon bacterial infection (Carrero et al., 2008). This observation is explained by a LLO-mediated apoptosis of T cells, an effect where granzymes are involved. Moreover, human cell lines loaded with granzyme A differ in their sensitivity to cytolysis (Beresford et al., 1999). Thus, the discrepancy between in vivo and in vitro killing capacity of *Sort1*$^{-/-}$ CTLs, as compared with WT animals, could be caused by the employment of different target cell lines as well. Alternatively,

the granzyme A increment observed in vitro might be too low to translate into an in vivo effect.

In accordance with the infection models, induction of IBD resulted in a milder colitis pathology in recipients of *Sort1*$^{-/-}$ CD4$^+$ T cells. The proinflammatory cytokine TNF-α is concurrently involved in IBD pathogenesis (Kojouharoff et al., 1997; Wirtz et al., 1999). However, TNF-α release was unaffected by loss of Sortilin; this finding may account for the colon lesions observed in *Sort1*$^{-/-}$ T cell recipients. Furthermore, unlike the complete penetrance of IFN-γ genetic deletion and the associated lack of an IBD phenotype (Ito and Fathman, 1997), in *Sort1*$^{-/-}$ mice IFN-γ release was strongly diminished but not ablated. We suggest that Sortilin modulates the adaptive and innate immune responses by regulating IFN-γ secretion.

Mechanistically, loss of Sortilin impaired release of IFN-γ-loaded carriers from the TGN. Consistent with the distribution of the sorting receptor in neurons (Vaegter et al., 2011; Willnow et al., 2008), the majority resided in the Golgi apparatus and in early endosomes. Thus, Sortilin would be in an ideal position to select soluble cargo molecules such as IFN-γ for inclusion into CCVs. We infer from our dynamic imaging experiments on IFN-γ and transferrin trafficking that during their itinerary, transferrin, Sortilin, and IFN-γ can pass through the same early endosomal structures, but might leave the endosomal sorting platform through different exit sites (Mari et al., 2008). During the post-early endosomal recycling phase, colocalization of transferrin and IFN-γ was lost, indicating that IFN-γ does not employ a recycling endosomal trafficking route for secretion. In activated Th1 cells, IFN-γ is released at the IS in a polarized fashion, whereas for TNF-α a multidirectional release has been suggested (Huse et al., 2006). We confirmed preferential orientation of IFN-γ around the IS. Transient costaining with Rab19$^+$ and recycling transferrin structures was observed along the post-Golgi trafficking route of IFN-γ; in contrast, Rab3d exhibited essentially no colocalization. Although there is a paucity of information about a specific role for Rab19 in exocytosis, Rab3d seems to control the size of secretory granules (Riedel et al., 2002).

In human NK cells, cotrafficking and multidirectional release of IFN-γ and TNF-α has been shown (Reefman et al., 2010). In contrast, in our study on murine CTLs and Th1 cells, Sortilin strongly influenced secretion of IFN-γ but not TNF-α, indicating that both cytokines employ separate secretory pathways. Differences between our findings and previous reports on murine Th1 cells and human NK cells include analysis of transfected T cells versus endogenously expressed cytokines and trafficking regulators.

Our data indicate that Sortilin provides a layer of selectivity for cargo molecules at the TGN. Loss of Sortilin strongly influenced secretion of IFN-γ and affected the availability of active granzyme A. At the TGN, Sortilin recruited IFN-γ into carriers destined for the early endosomal sorting platform, followed by IFN-γ sorting into a vesicle compartment that was distinct from recycling endosomes, late endosomes, and secretory lysosomes. IFN-γ has a dominant role in the modulation of the adaptive immune response after infections, tumor growth, and chronic inflammation (Kennedy and Celis, 2008). Thus, through IFN-γ trafficking, the sorting receptor gains a key role in maintaining systemic immune competence.

EXPERIMENTAL PROCEDURES

Adenovirus Infection

Mice were challenged by injection (i.v.) of 1 × 10^8 PFU of replication-deficient E1- and E3-deleted type 5 adenovirus encoding β-galactosidase (Lac-Z) (Willimsky and Blankenstein, 2000). On day 5 after challenge, 10 μg IFN-γ mAb per mouse were injected (i.p.). After 20 hr, concentration of IFN-γ in the serum was analyzed with mouse IFN-γ in vivo capture assay set (BD Bioscience). Serum concentration of IL-2 was determined by ELISA (BD Bioscience). To analyze frequencies of effector T cells, splenocytes from infected mice were restimulated with adenovirus-infected DCs (moi 20–50) overnight. For the final 4 hr BFA (10 μg/ml) was included. Splenocytes were stained for IFN-γ, CD4, and CD8, respectively, and then T cells were analyzed by flow cytometry. Liver damage was measured by quantifying the activity of the serum transaminases ALT and AST (LABOKLIN). Animal experiments were approved by the Berlin State review board at the Landesamt für Gesundheit und Soziales.

Listeria monocytogenes Infection

Mice were infected with the *L. monocytogenes* strain EGD essentially as previously described (Kursar et al., 2005). In brief, 5 × 10^3 bacteria in a volume of 200 μl PBS were injected into a lateral tail vein. Animals were sacrificed, and concentrations of IFN-γ and IL-2 in serum and tissue lysates were analyzed by ELISA or IFN-γ in vivo capture assay set. Peptide-specific restimulation to quantitate frequencies of antigen-specific T cells was performed essentially as described (Kursar et al., 2005). In brief, 4 × 10^6 cells were cultured for 4 hr in 1 ml complete RPMI including 5 μg/ml BFA, in the presence of 10^{-6} M of the peptide $LLO_{190-201}$ or in the presence of PMA and ionomycin. Cultured cells were then stained as described in Supplemental Experimental Procedures. For determination of bacterial burdens in spleen, mice were killed, tissues were homogenized in PBS, serial dilutions of homogenates were plated on tryptic soy broth plates, and colonies were counted after 48 hr of incubation at 30°C.

Induction of Inflammatory Bowel Disease

Flow cytometry-sorted 5 × 10^5 CD4$^+$CD25$^{lo/-}$ T cells were transferred intraperitoneally into *Rag2*$^{-/-}$ recipients. T cells were obtained from either *Sort1*$^{-/-}$ or C57BL/6 WT donors. In average, the purity of transferred CD4$^+$CD25$^{lo/-}$ T cells was in the range of 95% viable cells. Experimental animal groups were age and sex matched. Animals were monitored clinically for weight loss, and final evaluation was performed when mice lost 20% of their original body weight. Animals were euthanized, serum was generated, and colons were assessed histologically. Hematoxylin & eosin (H&E)-stained sections were scored blindly according to the criteria detailed in Supplemental Experimental Procedures.

Immunofluorescence

Cells were grown for 20 hr on poly-L-lysine-coated coverslips (Sigma). Cells were fixed with −20°C acetone or 3.5% PFA for 10 min on ice and washed with PBS. Subsequently, cells were permeabilized with 0.2% TX-100 in PBS for 5 min and blocked with 5% BSA in PBS for 30 min at room temperature. Next, cells were incubated with primary antibodies in 1% BSA in PBS for 1 hr at room temperature, washed, and exposed to a secondary fluorochrom-conjugated antibody for 45 min at room temperature. After washing, slides were mounted in Mowiol.

IFN-γ and Granzyme A Transport Assay

CTLs (day 5) were seeded on poly-L-lysine-coated coverslips for 2 hr at 19.5°C to accumulate IFN-γ and granzyme A and B in the Golgi, in the presence of 20 mM HEPES. Temperature was shifted to 37°C for up to 30 min (IFN-γ) and 45 min (granzyme A and B) in the presence of 40 μg/ml cycloheximide. Cells were fixed with −20°C acetone or ice-cold 3.5% PFA, permeabilized, and stained with specific antibodies. The ratio of IFN-γ fluorescence in the Golgi versus total cellular fluorescence was calculated at the indicated time points applying ImageJ software 1.43u. Confocal images are presented as medial single confocal sections. We performed also a three-dimensional reconstruction of a Z series of confocal optical sections taken at 0.075 μm intervals. For colocalization analysis of IFN-γ, granzyme A, and granzyme B, cells with an average signal of these antigens were picked at random. Six to ten planes with 0.4 μm increment of each cell were taken. The Mander's

overlap coefficient for each z stack was calculated with the LSM software ZEN (Zeiss).

Transferrin Transport Assay

CTLs were incubated with 20 μg/ml Alexa Fluor-488-labeled transferrin (Invitrogen) in RPMI with 2% FCS at 37°C for 30 min. The recycling phase was induced by washing the cells in ice-cold RPMI, followed by competition with excessive unlabeled transferrin (Sigma; 10× excess molar ratio) in RPMI with 10% FCS (4°C). Cells were seeded on coverslips, precoated with 3 μg/ml anti-CD3 and 2 μg/ml anti-CD28 for 15 min at 4°C, followed by a chase period at 37°C. Cells were fixed with 1% glutaraldehyde, permeabilized, and stained with the indicated antibodies. For colocalization analysis, cells with an average signal of Alexa Fluor 488-tagged transferrin were picked at random.

Laser Scanning Microscopy and Image Analysis

Confocal microscopy images of cells were acquired with a Zeiss LSM510Meta or LSM700 confocal setup on an Axiovert 200 M inverted microscope equipped with a three-line laser. Microscope settings and image processing are detailed in Supplemental Experimental Procedures.

Statistics

Results are expressed as mean ± SD or SEM, as indicated. Data were considered statistically significant for $p \leq 0.05$, which was determined by Wilcoxon signed rank test, Mann-Whitney test, or two-tailed unpaired Student's t test as indicated.

SUPPLEMENTAL INFORMATION

Supplemental Information includes Supplemental Experimental Procedures, five figures, and two movies and can be found with this article online at http://dx.doi.org/10.1016/j.immuni.2012.07.012.

ACKNOWLEDGMENTS

We thank A. Nykjaer for providing *Sort1*$^{-/-}$ mice. We are indebted to M. Schaefer, C. Brettschneider, A. Bauerfeind, A. Sporbert, H.-P. Rahn, and V. Schumacher for expert technical advice or assistance. I. Morano generously provided us with recombinant adenovirus. We are grateful to J. Klumperman and O. Daumke for helpful discussions.

Received: July 20, 2011
Accepted: July 20, 2012
Published online: October 18, 2012

REFERENCES

Andersson, A., Dai, W.J., Di Santo, J.P., and Brombacher, F. (1998). Early IFN-gamma production and innate immunity during *Listeria monocytogenes* infection in the absence of NK cells. J. Immunol. *161*, 5600–5606.

Antonin, W., Holroyd, C., Fasshauer, D., Pabst, S., Von Mollard, G.F., and Jahn, R. (2000). A SNARE complex mediating fusion of late endosomes defines conserved properties of SNARE structure and function. EMBO J. *19*, 6453–6464.

Beresford, P.J., Xia, Z., Greenberg, A.H., and Lieberman, J. (1999). Granzyme A loading induces rapid cytolysis and a novel form of DNA damage independently of caspase activation. Immunity *10*, 585–594.

Canuel, M., Lefrancois, S., Zeng, J., and Morales, C.R. (2008). AP-1 and retromer play opposite roles in the trafficking of sortilin between the Golgi apparatus and the lysosomes. Biochem. Biophys. Res. Commun. *366*, 724–730.

Carrero, J.A., Vivanco-Cid, H., and Unanue, E.R. (2008). Granzymes drive a rapid listeriolysin O-induced T cell apoptosis. J. Immunol. *181*, 1365–1374.

Catalfamo, M., Karpova, T., McNally, J., Costes, S.V., Lockett, S.J., Bos, E., Peters, P.J., and Henkart, P.A. (2004). Human CD8+ T cells store RANTES in a unique secretory compartment and release it rapidly after TcR stimulation. Immunity *20*, 219–230.

Clark, R.H., Stinchcombe, J.C., Day, A., Blott, E., Booth, S., Bossi, G., Hamblin, T., Davies, E.G., and Griffiths, G.M. (2003). Adaptor protein 3-dependent microtubule-mediated movement of lytic granules to the immunological synapse. Nat. Immunol. *4*, 1111–1120.

Dell'Angelica, E.C., Shotelersuk, V., Aguilar, R.C., Gahl, W.A., and Bonifacino, J.S. (1999). Altered trafficking of lysosomal proteins in Hermansky-Pudlak syndrome due to mutations in the beta 3A subunit of the AP-3 adaptor. Mol. Cell *3*, 11–21.

Ebnet, K., Hausmann, M., Lehmann-Grube, F., Müllbacher, A., Kopf, M., Lamers, M., and Simon, M.M. (1995). Granzyme A-deficient mice retain potent cell-mediated cytotoxicity. EMBO J. *14*, 4230–4239.

Evans, S.F., Irmady, K., Ostrow, K., Kim, T., Nykjaer, A., Saftig, P., Blobel, C., and Hempstead, B.L. (2011). Neuronal brain-derived neurotrophic factor is synthesized in excess, with levels regulated by sortilin-mediated trafficking and lysosomal degradation. J. Biol. Chem. *286*, 29556–29567.

Fooksman, D.R., Vardhana, S., Vasiliver-Shamis, G., Liese, J., Blair, D.A., Waite, J., Sacristán, C., Victora, G.D., Zanin-Zhorov, A., and Dustin, M.L. (2010). Functional anatomy of T cell activation and synapse formation. Annu. Rev. Immunol. *28*, 79–105.

Fortier, A.H., Nacy, C.A., and Sitkovsky, M.V. (1989). Similar molecular requirements for antigen receptor-triggered secretion of interferon and granule enzymes by cytolytic T lymphocytes. Cell. Immunol. *124*, 64–76.

Ghosh, P., Dahms, N.M., and Kornfeld, S. (2003). Mannose 6-phosphate receptors: new twists in the tale. Nat. Rev. Mol. Cell Biol. *4*, 202–212.

Huang, S., Hendriks, W., Althage, A., Hemmi, S., Bluethmann, H., Kamijo, R., Vilcek, J., Zinkernagel, R.M., and Aguet, M. (1993). Immune response in mice that lack the interferon-gamma receptor. Science *259*, 1742–1745.

Huse, M., Lillemeier, B.F., Kuhns, M.S., Chen, D.S., and Davis, M.M. (2006). T cells use two directionally distinct pathways for cytokine secretion. Nat. Immunol. *7*, 247–255.

Ito, H., and Fathman, C.G. (1997). CD45RBhigh CD4+ T cells from IFN-gamma knockout mice do not induce wasting disease. J. Autoimmun. *10*, 455–459.

Kennedy, R., and Celis, E. (2008). Multiple roles for CD4+ T cells in anti-tumor immune responses. Immunol. Rev. *222*, 129–144.

Kojouharoff, G., Hans, W., Obermeier, F., Männel, D.N., Andus, T., Schölmerich, J., Gross, V., and Falk, W. (1997). Neutralization of tumour necrosis factor (TNF) but not of IL-1 reduces inflammation in chronic dextran sulphate sodium-induced colitis in mice. Clin. Exp. Immunol. *107*, 353–358.

Krzewski, K., Gil-Krzewska, A., Watts, J., Stern, J.N., and Strominger, J.L. (2011). VAMP4- and VAMP7-expressing vesicles are both required for cytotoxic granule exocytosis in NK cells. Eur. J. Immunol. *41*, 3323–3329.

Kursar, M., Höpken, U.E., Koch, M., Köhler, A., Lipp, M., Kaufmann, S.H., and Mittrücker, H.W. (2005). Differential requirements for the chemokine receptor CCR7 in T cell activation during *Listeria monocytogenes* infection. J. Exp. Med. *201*, 1447–1457.

Marcet-Palacios, M., Odemuyiwa, S.O., Coughlin, J.J., Garofoli, D., Ewen, C., Davidson, C.E., Ghaffari, M., Kane, K.P., Lacy, P., Logan, M.R., et al. (2008). Vesicle-associated membrane protein 7 (VAMP-7) is essential for target cell killing in a natural killer cell line. Biochem. Biophys. Res. Commun. *366*, 617–623.

Mari, M., Bujny, M.V., Zeuschner, D., Geerts, W.J., Griffith, J., Petersen, C.M., Cullen, P.J., Klumperman, J., and Geuze, H.J. (2008). SNX1 defines an early endosomal recycling exit for sortilin and mannose 6-phosphate receptors. Traffic *9*, 380–393.

Poe, M., Wu, J.K., Blake, J.T., Zweerink, H.J., and Sigal, N.H. (1991). The enzymatic activity of human cytotoxic T-lymphocyte granzyme A and cytolysis mediated by cytotoxic T-lymphocytes are potently inhibited by a synthetic antiprotease, FUT-175. Arch. Biochem. Biophys. *284*, 215–218.

Pryor, P.R., Mullock, B.M., Bright, N.A., Lindsay, M.R., Gray, S.R., Richardson, S.C., Stewart, A., James, D.E., Piper, R.C., and Luzio, J.P. (2004). Combinatorial SNARE complexes with VAMP7 or VAMP8 define different late endocytic fusion events. EMBO Rep. *5*, 590–595.

Reefman, E., Kay, J.G., Wood, S.M., Offenhäuser, C., Brown, D.L., Roy, S., Stanley, A.C., Low, P.C., Manderson, A.P., and Stow, J.L. (2010). Cytokine

secretion is distinct from secretion of cytotoxic granules in NK cells. J. Immunol. *184*, 4852–4862.

Riedel, D., Antonin, W., Fernandez-Chacon, R., Alvarez de Toledo, G., Jo, T., Geppert, M., Valentijn, J.A., Valentijn, K., Jamieson, J.D., Südhof, T.C., and Jahn, R. (2002). Rab3D is not required for exocrine exocytosis but for maintenance of normally sized secretory granules. Mol. Cell. Biol. *22*, 6487–6497.

Robinson, M.S., and Bonifacino, J.S. (2001). Adaptor-related proteins. Curr. Opin. Cell Biol. *13*, 444–453.

Rous, B.A., Reaves, B.J., Ihrke, G., Briggs, J.A., Gray, S.R., Stephens, D.J., Banting, G., and Luzio, J.P. (2002). Role of adaptor complex AP-3 in targeting wild-type and mutated CD63 to lysosomes. Mol. Biol. Cell *13*, 1071–1082.

Rüder, C., Höpken, U.E., Wolf, J., Mittrücker, H.W., Engels, B., Erdmann, B., Wollenzin, S., Uckert, W., Dörken, B., and Rehm, A. (2009). The tumor-associated antigen EBAG9 negatively regulates the cytolytic capacity of mouse CD8+ T cells. J. Clin. Invest. *119*, 2184–2203.

Russell, J.H., and Ley, T.J. (2002). Lymphocyte-mediated cytotoxicity. Annu. Rev. Immunol. *20*, 323–370.

Schneider, M.A., Meingassner, J.G., Lipp, M., Moore, H.D., and Rot, A. (2007). CCR7 is required for the in vivo function of CD4+ CD25+ regulatory T cells. J. Exp. Med. *204*, 735–745.

Stetson, D.B., Mohrs, M., Reinhardt, R.L., Baron, J.L., Wang, Z.E., Gapin, L., Kronenberg, M., and Locksley, R.M. (2003). Constitutive cytokine mRNAs mark natural killer (NK) and NK T cells poised for rapid effector function. J. Exp. Med. *198*, 1069–1076.

Stinchcombe, J., Bossi, G., and Griffiths, G.M. (2004). Linking albinism and immunity: the secrets of secretory lysosomes. Science *305*, 55–59.

Sung, R.S., Qin, L., and Bromberg, J.S. (2001). TNFalpha and IFNgamma induced by innate anti-adenoviral immune responses inhibit adenovirus-mediated transgene expression. Mol. Ther. *3*, 757–767.

Trapani, J.A. (2001). Granzymes: a family of lymphocyte granule serine proteases. Genome Biol. *2*, REVIEWS3014.

Vaegter, C.B., Jansen, P., Fjorback, A.W., Glerup, S., Skeldal, S., Kjolby, M., Richner, M., Erdmann, B., Nyengaard, J.R., Tessarollo, L., et al. (2011). Sortilin associates with Trk receptors to enhance anterograde transport and neurotrophin signaling. Nat. Neurosci. *14*, 54–61.

Voskoboinik, I., Smyth, M.J., and Trapani, J.A. (2006). Perforin-mediated target-cell death and immune homeostasis. Nat. Rev. Immunol. *6*, 940–952.

Willimsky, G., and Blankenstein, T. (2000). Interleukin-7/B7.1-encoding adenoviruses induce rejection of transplanted but not nontransplanted tumors. Cancer Res. *60*, 685–692.

Willnow, T.E., Petersen, C.M., and Nykjaer, A. (2008). VPS10P-domain receptors - regulators of neuronal viability and function. Nat. Rev. Neurosci. *9*, 899–909.

Wirtz, S., Finotto, S., Kanzler, S., Lohse, A.W., Blessing, M., Lehr, H.A., Galle, P.R., and Neurath, M.F. (1999). Cutting edge: chronic intestinal inflammation in STAT-4 transgenic mice: characterization of disease and adoptive transfer by TNF- plus IFN-gamma-producing CD4+ T cells that respond to bacterial antigens. J. Immunol. *162*, 1884–1888.

Yang, Y., Ertl, H.C., and Wilson, J.M. (1994). MHC class I-restricted cytotoxic T lymphocytes to viral antigens destroy hepatocytes in mice infected with E1-deleted recombinant adenoviruses. Immunity *1*, 433–442.